

An Enhanced Automatic Algorithm for Estimation of Respiratory Variations in Arterial Pulse Pressure During Regions of Abrupt Hemodynamic Changes

Mateo Aboy*, *Member, IEEE*, Cristina Crespo, and Daniel Austin, *Member, IEEE*

Abstract—We describe an improved automatic algorithm to estimate the pulse-pressure-variation (PPV) index from arterial blood pressure (ABP) signals. This enhanced algorithm enables for PPV estimation during periods of abrupt hemodynamic changes. Numerous studies have shown PPV to be one of most specific and sensitive predictors of fluid responsiveness in mechanically ventilated patients. The algorithm uses a beat detection algorithm to perform beat segmentation, kernel smoothers for envelope detection, and a suboptimal Kalman filter for PPV estimation and artifact removal. In this paper, we provide a detailed description of the algorithm and assess its performance on over 40 h of ABP signals obtained from 18 mechanically ventilated crossbred Yorkshire swine. The subjects underwent grade V liver injury after splenectomy, while receiving mechanical ventilation, and general anesthesia with isoflurane. All subjects in the database underwent a period of abrupt hemodynamic change after an induced grade V liver injury involving severe blood loss resulting in hemorrhagic shock, followed by fluid resuscitation with either 0.9% normal saline or lactated ringers solutions. Trained experts manually calculated PPV at five time instances during the period of abrupt hemodynamic changes. We report validation results comparing the proposed algorithm against a commercial system (pulse contour cardiac output, PICCO) with continuous PPV monitoring capabilities. Both systems were assessed during periods of abrupt hemodynamic changes against the “gold-standard” PPV, calculated and manually annotated by experts. Our results indicate that the proposed algorithm performs considerably better than the PICCO system during regions of abrupt hemodynamic changes.

Index Terms—Fluid responsiveness, hemodynamic monitoring, pulse contour cardiac output (PICCO), pulse contour analysis, pulse-pressure-variation (PPV) index (PPV), stroke-volume-variation index (SSV).

I. INTRODUCTION

WE DESCRIBE a novel automatic algorithm that can be used to obtain the pulse-pressure-variation (PPV) index from arterial blood pressure (ABP) signals. This enhanced

Manuscript received November 8, 2008; revised February 4, 2009 and May 10, 2009. First published June 16, 2009; current version published September 16, 2009. *Asterisk indicates corresponding author.*

*M. Aboy is with the Electrical Engineering Department, Oregon Institute of Technology (OIT), Portland, OR 97006 USA, and also with the University of London, London WC1E 7HU, U.K. (e-mail: mateoaboy@ieee.org).

C. Crespo is with the Electrical Engineering Department, Oregon Institute of Technology (OIT), Portland, OR 97006 USA, and also with the School of Telecommunications Engineers (ETSIT-Vigo), University of Vigo, Vigo 36310, Spain.

D. Austin is with the Electrical Engineering Department, Oregon Institute of Technology (OIT), Portland, OR 97006 USA, and also with Portland State University (PSU), Portland, OR 97207 USA. He is also with the Biomedical Engineering Division, Oregon Health and Science University, Portland, OR 97239 USA.

Digital Object Identifier 10.1109/TBME.2009.2024761

algorithm is designed to be capable of estimating PPV during regions of abrupt hemodynamic changes and artifact. Numerous studies have demonstrated that PPV is one of the most sensitive and specific predictors of fluid responsiveness. Specifically, PPV has been shown to be useful as a dynamic indicator to guide fluid therapy in different patient populations receiving mechanical ventilation [1]. For instance, PPV was found to exhibit better performance as a predictor of fluid responsiveness in patients before off-pump coronary artery bypass grafting than standard static preload indexes [2]. PPV has also been shown to be useful for predicting and assessing the hemodynamic effects of volume expansion and a reliable predictor of fluid responsiveness in mechanically ventilated patients with acute circulatory failure related to sepsis [3], [4]. Another study concluded that PPV can be used to predict whether or not volume expansion will increase cardiac output in postoperative patients who have undergone coronary artery bypass grafting [5]. A critical review of studies investigating predictive factors of fluid responsiveness in intensive care unit patients concluded that PPV and other dynamic parameters should be used preferentially to static parameters to predict fluid responsiveness [6].

The standard method for calculating PPV often requires simultaneous recording of arterial and airway pressure. Pulse pressure (PP) is calculated on a beat-to-beat basis as the difference between systolic and diastolic arterial pressure. Maximal PP (PP_{\max}) and minimal PP (PP_{\min}) are calculated over a single respiratory cycle, which is determined from the airway pressure signal. PPVs ΔPP are calculated in terms of PP_{\max} and PP_{\min} , and expressed as a percentage

$$PPV(\%) = 100 \times \frac{PP_{\max} - PP_{\min}}{(PP_{\max} + PP_{\min})/2}. \quad (1)$$

We describe an enhanced algorithm to evaluate PPV from ABP signals and assess its performance of real ABP recordings. A previous version of the algorithm has been previously described [7]. This previous algorithm was made publicly available by the authors and due to its performance has been adopted by Philips Medical Systems. Currently, our previously published PPV algorithm is displayed in real time on the Philips Intellivue MP70 monitors (Intellivue MP70, Philips Medical Systems) and has been used in numerous studies related to PPV and fluid responsiveness. Its ability to monitor fluid responsiveness in the operating room and its accuracy against the gold standard obtained by manual annotations were assessed by Cannesson *et al.* [8]. Respiratory variations in arterial PP (PPVman) are accurate predictors of fluid responsiveness in mechanically

ventilated patients. However, they cannot be continuously monitored. Thus, in their study they assessed the clinical utility of our previously published automatic estimation algorithm of PPV (PPVauto). Their results showed that the agreement between PPVman (gold-standard PPV through manual annotations) and our PPVauto over the 200 pairs of collected data was $0.7\% \pm 3.4\%$ (mean bias \pm sd). A total of 17 patients were responders to volume expansion. A threshold PPVman value of 12% allowed discrimination of responders to volume expansion with a sensitivity of 88% and a specificity of 100%, and a threshold PPVauto value of 10% allowed discrimination of responders to volume expansion with a sensitivity of 82% and a specificity of 88%. Thus, they concluded that our previous automatic PPV algorithm, PPVauto, is strongly correlated to PPman, is an accurate predictor of fluid responsiveness, and allows continuous monitoring of PPV. As stated by Cannesson *et al.* [8], PPV is still considered the best predictor of fluid responsiveness in this setting. However, it previously was not possible to conveniently monitor this index in the operating room or in the intensive care unit. Thus, the automatic PPV has potential clinical application for fluid management optimization in the operating room. Cannesson has made significant contributions related to fluid responsiveness based on dynamic indicators such as PPV [9]–[11]

A limitation of our previously described [7] algorithm adopted by Philips in their Intelliveu MP70 monitors is that it may not work adequately in regions of abrupt hemodynamic changes. In this paper, we provide a detailed description of an improved algorithm that contains additional filters in order to make it robust to abrupt hemodynamic changes and assess its performance on over 40 h of ABP recordings from 18 different subjects. We report validation results comparing the proposed improved algorithm against a commercial system with continuous PPV monitoring capabilities (PICCO Pulsion Medical Systems, Munich, Germany). Both systems were assessed during periods of abrupt hemodynamic changes against the “gold-standard” PPV, calculated and manually annotated by experts. The pulse contour cardiac output (PICCO) physiological monitor has been used extensively in research studies for hemodynamic monitoring [2], [12]–[30]. Despite the availability of a commercial device for PPV monitoring, the need for additional independent PPV estimation algorithms is significant for several reasons. For instance, the results of one of these studies suggested that the PICCO PPV algorithm may not work well in certain situations [29] and our validation results indicate that the PICCO system may not work well during regions of abrupt hemodynamic changes. Second, the improved PPV algorithm presented in this paper can be implemented and used to estimate PPV in data already collected and archived. Finally, we provide a detailed description to ensure that other researchers and medical manufacturers can implement it and use it for research purposes, and to independently validate the results obtained using commercial PPV monitoring systems. As was the case with our previous version of the algorithm adopted by Philips Medical Systems, we provide a thorough description designed to ensure reproducibility so that both medical manufacturers such as Philips and Pulsion or independent researcher can implement it as part of their commercial systems.

II. METHODS: ALGORITHM DESCRIPTION

In this section, we provide a detailed description of the enhanced PPV estimation algorithm designed to improve its robustness during regions of abrupt hemodynamic change and artifact. The methodology for steps 1–3 shortly is not identical but equivalent to [7, steps 1–5]. We provide an abbreviated description of these steps for completeness.

A. Step 1: Beat Detection and Segmentation

An automatic beat detection algorithm for pressure signals is applied to the input pressure signal $x(n)$ to identify the time instance corresponding to the beginning of each beat

$$\mathbf{a} = f(x(n)) \quad (2)$$

where $f(x(n))$ denotes the operation of applying the detection algorithm to the input signal $x(n)$. The result of this operation is a vector \mathbf{a} that contains the sample indexes corresponding to the beginning of each beat (i.e., the minima preceding each beat)

$$\mathbf{a} = (a_1, a_2, \dots, a_N). \quad (3)$$

Based on the vector $\mathbf{a} = (a_1, a_2, \dots, a_N)$, the data are segmented as a set of N vectors corresponding to the N beats present in the signal

$$\begin{aligned} \mathbf{x}_1 &= (x(a_1), x(a_1 + 1), \dots, x(a_2 - 1)) \\ \mathbf{x}_2 &= (x(a_2), x(a_2 + 1), \dots, x(a_3 - 1)) \\ &\vdots \\ \mathbf{x}_N &= (x(a_N), x(a_N + 1), \dots, x(L)) \end{aligned} \quad (4)$$

where $x(L)$ denotes the last sample in $x(n)$.

In this implementation, we used the detection algorithm described in [31]. In practice, any automatic detection algorithm with good performance can be used to perform this task. It should also be noted that this is a different detection algorithm than that used in [7].

B. Step 2: Beat Maxima Detection

Given the set of vectors $\{\mathbf{x}_k\}_{k=1}^N$ corresponding to the segmented signal $x(n)$, the algorithm detects the time index b_k corresponding the maximum in each segment

$$\begin{aligned} b_1 &= \arg \max_{a_1 < n < a_2 - 1} \mathbf{x}_1 \\ b_2 &= \arg \max_{a_2 < n < a_3 - 1} \mathbf{x}_2 \\ &\vdots \\ b_N &= \arg \max_{a_N < n < L} \mathbf{x}_N. \end{aligned} \quad (5)$$

The result of this step is a vector \mathbf{b} that contains the sample indexes corresponding to the maxima of each beat

$$\mathbf{b} = \arg \max_{a_i < n < a_{i+1} - 1} \{\mathbf{x}\}_{k=1}^N = (b_1, b_2, \dots, b_N). \quad (6)$$

C. Step 3: Envelope Estimation

In the next step, the algorithm estimates the upper $u_e(n)$ and lower $l_e(n)$ envelopes from the $x(\mathbf{b})$ and $x(\mathbf{a})$ time series, respectively. This is accomplished by smoothing and uniformly resampling $x(\mathbf{a})$ and $x(\mathbf{b})$ at a rate of f_s with a kernel smoother

$$u_e(n) = \frac{\sum_{k=1}^N x(\mathbf{b})b(|nT_s - t(k)|/\sigma_b)}{\sum_{k=1}^N b(|nT_s - t(k)|/\sigma_b)} \quad (7)$$

$$l_e(n) = \frac{\sum_{k=1}^N x(\mathbf{a})b(|nT_s - t(k)|/\sigma_b)}{\sum_{k=1}^N b(|nT_s - t(k)|/\sigma_b)} \quad (8)$$

where $T_s = 1/f_s$ is the resampling interval with f_s corresponding to the original sampling frequency of $x(n)$, $t(k)$ denotes the times of the signal observations, σ_b is the kernel width, and $b(\cdot)$ is a clipped Gaussian kernel function

$$b(u) = \begin{cases} \exp\left(\frac{-u^2}{2}\right), & \text{if } -5 \leq u \leq 5 \\ 0, & \text{otherwise.} \end{cases} \quad (9)$$

The kernel width controls the degree of smoothing and depends on the fundamental frequency of the pressure signal (heart rate). A width of 0.2 s works well for heart rates up to 4 Hz.

D. Step 4: PPV Estimation

The algorithm uses the estimated upper $u_e(n)$ and lower $l_e(n)$ envelopes to obtain a continuous estimate of the PP

$$r(n) = u_e(n) - l_e(n). \quad (10)$$

The estimate of PP $r(n)$ also serves as an estimate of the respiratory signal during mechanical ventilation.

A PP data matrix $\mathbf{R} = (\mathbf{r}_1, \mathbf{r}_2, \dots, \mathbf{r}_M)$ is created by partitioning the PP signal $r(n)$ into M 50% overlapping vectors of dimension $D = 2(1/f_r)f_s \times 1$

$$M = 2T_r \frac{2L}{f_s} \quad (11)$$

where $T_r = 1/f_r$ is the average respiratory period and f_r the respiratory frequency, L denotes the number of samples in $x(n)$, $u_e(n)$, $l_e(n)$ and $r(n)$, and f_s is the sampling frequency.

Given the set of vectors $\{\mathbf{r}_k\}_{k=1}^M$, the algorithm detects the time index c_k corresponding the minimum in each segment

$$\begin{aligned} c_1 &= \arg \min_{1 < n < D} \mathbf{r}_1 \\ c_2 &= \arg \min_{1 < n < D} \mathbf{r}_2 \\ &\vdots \\ c_M &= \arg \min_{1 < n < D} \mathbf{r}_M. \end{aligned} \quad (12)$$

The result of this step is a vector \mathbf{c} that contains the sample indexes corresponding to the minima of each \mathbf{r} ,

$$\mathbf{c} = \arg \min_{1 < n < D} \{\mathbf{r}\}_{k=1}^M = (c_1, c_2, \dots, c_M). \quad (13)$$

Analogously, the algorithm detects the time index d_k corresponding the maximum for each vector \mathbf{r}

$$\mathbf{d} = \arg \max_{1 < n < D} \{\mathbf{r}\}_{k=1}^M = (d_1, d_2, \dots, d_M). \quad (14)$$

The raw PPV index \mathbf{y} is obtained from the \mathbf{c} and \mathbf{d} vectors

$$\mathbf{y} = 2 \frac{x(\mathbf{d}) - x(\mathbf{c})}{x(\mathbf{d}) + x(\mathbf{c})} = 2\mathbf{m} \quad (15)$$

where \mathbf{m} denotes the amplitude-modulation (AM) index defined for large carrier double side-band AM.

The \mathbf{y} vector may contain erroneous values in regions where the input pressure signal $x(n)$ is corrupted by artifact. Thus, the final estimate of the PPV index $\hat{\mathbf{p}}$ is obtained by applying a recursive filter to process the raw measurements \mathbf{y}

$$\hat{p}_{n+1|n+1} = \hat{p}_{n+1|n} + K_{n+1}(y_{n+1} - \hat{p}_{n+1|n}) \quad (16)$$

Domain knowledge about the evolution of the true PPV \mathbf{p} is incorporated into the estimator by constraining the PPV index to evolve slowly

$$p_{n+1} = p_n + u_n \quad (17)$$

i.e., the PPV index at time $n+1$, p_{n+1} , is equal to the pressure variation index at the previous time n , p_n , within some error u_n .

The gain K_{n+1} is a function of the difference between the measured and the estimated PPV index based on the model, $e_{n+1} = y_{n+1} - \hat{p}_{n+1|n}$

$$K_{n+1} = \begin{cases} \kappa_1, & \text{if } |e_{n+1}| = |y_{n+1} - \hat{p}_{n+1|n}| \leq \xi_1 \\ \kappa_2, & \text{if } \xi_1 \leq |e_{n+1}| = |y_{n+1} - \hat{p}_{n+1|n}| \leq \xi_2 \\ \kappa_3, & \text{if } |e_{n+1}| = |y_{n+1} - \hat{p}_{n+1|n}| \geq \xi_2 \end{cases} \quad (18)$$

where the vectors $\mathbf{K} = (\kappa_1, \kappa_2, \kappa_3)$ and $\mathbf{T} = (\xi_1, \xi_2)$ are user-specified parameters. By default, our algorithm implementation uses $\mathbf{K} = (1, 0.5, 0)$ and $\mathbf{T} = (1, 25)$. For these specific \mathbf{K} and \mathbf{T} , the algorithm discards PPV measurements \mathbf{y} when the residual $|e_{n+1}| = |y_{n+1} - \hat{p}_{n+1|n}| \geq \xi_2$, since the PPV is not supposed to change so significantly from one respiratory cycle to the next. Analogously, the algorithm updates the predicted PPV based on the model using the measurements \mathbf{y} when $|e_{n+1}| = |y_{n+1} - \hat{p}_{n+1|n}| \leq \xi_1$, since this variability can be considered physiological in nature. For values of the residual $\xi_1 \leq |e_{n+1}| \leq \xi_2$, the predicted PPV based on the model $\hat{p}_{n+1|n}$ is updated by $\kappa_2 e_{n+1} = 0.5e_{n+1}$.

Note that this recursive filter implements a Kalman filter where the state $p_{n+1} = p_n + u_n$ is modeled as a slowly changing process, and the noisy measurements are linearly related to the state $y_{n+1} = p_n + v_n$. However, the Kalman gains K_{n+1} are not computed based on the error covariance matrix and are only approximate. Thus, the piecewise constant gains $\mathbf{K} = (\kappa_1, \kappa_2, \kappa_3)$ are suboptimal.

III. ALGORITHM ASSESSMENT

The proposed enhanced algorithm was compared against a commercial PPV monitoring system (PICCO Pulsion Medical

TABLE I
 DETAILS FOR THE ANIMAL STUDY INCLUDING WEIGHT (WT), BLOOD LOSS DURING INJURY (EBL_INJ), BLOOD LOSS DURING RESUSCITATION (EBL_RES), CHANGE IN PPV, CARDIAC OUTPUT (CO), AND GLOBAL END-DIASTOLIC (GEDV) VALUES AT BASELINE (BASELINE), DURING INJURY AFTER THE BLEEDING STOPPED (BLEED STOP), AND AFTER POSTRESUSCITATION (POST RESUS) ARE SHOWN

SUBJECT Id.	WT (KG)	EBL_INJ (ML)	EBL_RES (ML)	CHANGE PPV INJ (%)	BASELINE CO (L/MIN)	BLEED STOP CO (L/MIN)	POST RESUS CO (L/MIN)	BASELINE GEDV (ML)	BLEED STOP GEDV (ML)	POST RESUS GEDV (ML)
Subj. 1	34.4	537.2	66.4	57.5	2.7	2.2	4.9	494	401	548
Subj. 2	39.0	494.9	37.6	36.7	2.7	1.7	3.6	421	327	443
Subj. 3	37.5	595.9	247.6	42.1	2.0	1.7	5.6	473	339	505
Subj. 4	38.0	883.2	324.9	43.8	3.7	2.7	5.8	539	392	521
Subj. 5	32.8	563.5	625.8	45.8	3.3	2.2	6.7	449	363	557
Subj. 6	35.0	543.2	135.8	27.6	3.2	2.5	5.3	461	442	513
Subj. 7	36.2	555.0	136.2	55.2	--	2.1	6.1	--	358	481
Subj. 8	37.3	642.6	484.5	67.4	3.3	2.2	4.6	463	375	423
Subj. 9	39.8	869.5	116.6	59.8	3.1	2.2	5.0	551	424	578
Subj. 10	36.2	763.6	302.3	30.4	2.6	2.2	5.1	590	488	612
Subj. 11	34.8	776.2	513.1	49.8	2.1	1.6	3.9	528	392	539
Subj. 12	33.4	844.6	86.3	49.8	2.8	2.0	2.9	485	461	430
Subj. 13	32.7	513.5	315.5	36.5	2.7	2.1	4.9	518	385	564
Subj. 14	34.2	1124.3	485.7	49.5	4.4	1.4	6.6	557	342	617
Subj. 15	30.5	896.3	216.2	49.2	2.3	1.3	4.6	470	259	430
Subj. 16	32.6	416.4	324.3	45.8	2.8	2.4	4.0	490	394	443
Subj. 17	32.8	850.9	292.0	51.1	2.8	1.8	7.0	475	276	511
Subj. 18	26.2	583.0	332.6	73.7	2.2	2.0	5.6	382	299	446
Mean	34.6	691.9	280.2	48.4	2.9	2.0	5.1	490	373	508
± SD	± 3.3	± 189.3	± 168.4	± 11.8	± 0.6	± 0.4	± 1.1	± 52	± 60	± 63

Systems) and validated prospectively against expert-annotated ABP signals. The algorithm was developed using pressure signals from different subjects than those used for performance assessment. The assessment was measured only once without any parameter tuning. It is important to note that the underlying algorithm has already been thoroughly assessed as part of a clinical study by Cannesson *et al.* [8]. Thus, our objective is not to conduct a clinical assessment regarding fluid responsiveness or to produce Bland–Altman plots of the algorithm against manually annotated PPV. For this, we refer our readers to [8]. Instead our objective is to present the performance of the algorithm compared to a commercial systems during regions of abrupt hemodynamic changes.

The database used for our study was composed of 18 ABP signals sampled at 50 Hz obtained from 18 mechanically ventilated crossbred Yorkshire swine (over 40 h of ABP recordings). These recordings were acquired at the Animal Laboratory of the Oregon Health and Science University (Portland, OR). The subjects underwent grade V liver injury after splenectomy, while receiving mechanical ventilation, and general anesthesia with isoflurane. All subjects in the database underwent a period of abrupt hemodynamic change after an induced grade V liver injury involving severe blood loss resulting in hemorrhagic shock, followed by fluid resuscitation with either 0.9% normal saline or lactated ringers solutions. Trained experts manually calculated PPV at five time instances during the period of abrupt hemodynamic changes. These expert manual annotations provide a “gold-standard” for algorithm comparison and validation. Table I shows the details of the animal study. The study protocol was reviewed and approved by the Institutional Review Board at Oregon Health and Science University.

IV. RESULTS AND DISCUSSION

Fig. 1 shows a comparison of the proposed enhanced PPV algorithm (dark grey) against a commercial PPV monitoring system (light grey) for two of the first nine subjects (subjects 1 and 3 where the PICCO system performed best, as listed in Table II). For each subject the top plot shows the ABP signal and the bottom plot shows the estimated PPV using both algorithms. Five “gold-standard” PPV manual annotations calculated by trained experts during periods of abrupt ABP changes are shown as black squares on the bottom plot of each subject. Note that both systems are consistent for the most part during periods where the ABP signal is relatively stationary. The proposed algorithm has better performance than the commercial PPV monitoring system during periods of abrupt ABPM changes. Fig. 2 shows the same type of figure for subjects 2, 4, 5, 13, 15, and 19.

Figs. 1(a) and 2(a) show examples where the ABP signal was severely corrupted by artifact. In these cases, the commercial PPV system fails to provide an adequate PPV value. Note, however, how the proposed enhanced algorithm is robust to these types of artifact. In these regions, the algorithm discards the PPV measurements y because the residual $|e_{n+1}| = |y_{n+1} - \hat{p}_{n+1|n}| \geq \xi_2$. Since the PPV is not supposed to change so significantly from one respiratory cycle to the next, the algorithm performs a time update (model-based prediction) and no measurement update.

The PICCO system performed well in regions of normal hemodynamic changes. However, its algorithm failed to accurately estimate the PPV during the periods between the injury and fluid resuscitation in all the subjects, and consequently, it failed to predict fluid responsiveness during the periods of severe

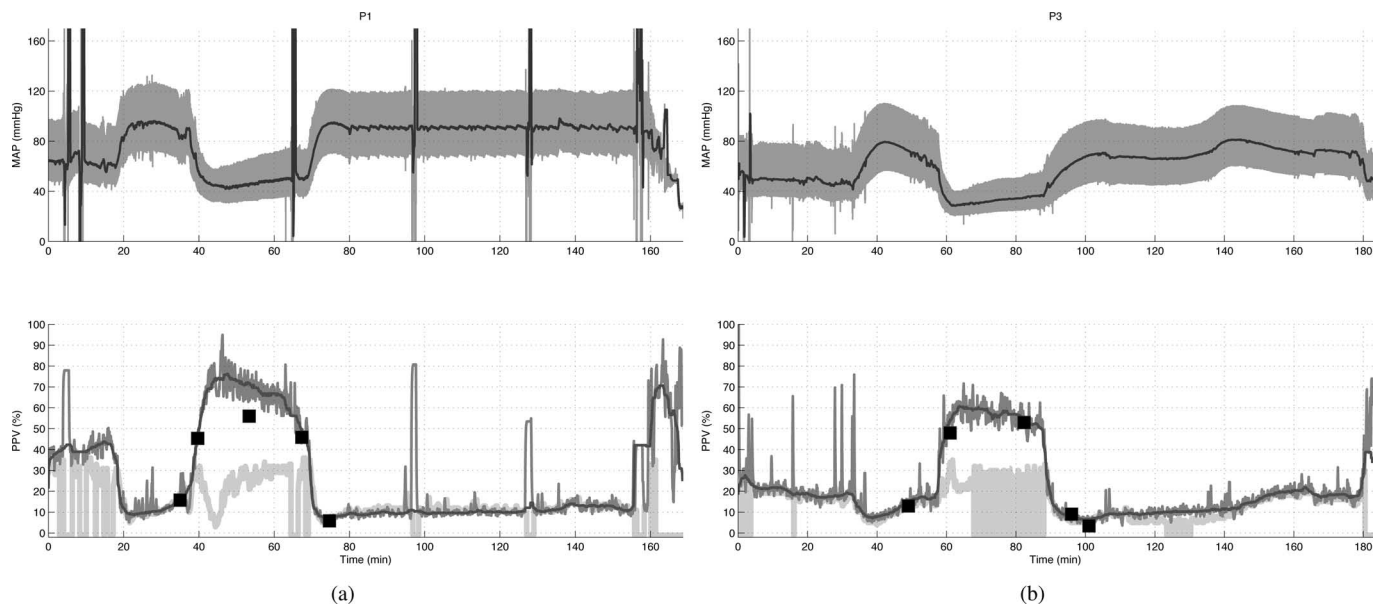


Fig. 1. Comparison of (bottom plot, dark grey) proposed enhanced PPV algorithm against (bottom, light grey) commercial PPV monitoring system for subjects (a) 1 and (b) 3 listed in Table II. The PICCO system had the best performance on these two subjects. For each subject, the top plot shows the ABP signal and the bottom plot shows the estimated PPV using both algorithms. Five “gold-standard” PPV manual annotations calculated by trained experts during periods of abrupt ABP changes are shown as black squares on the bottom plot of each subject. Note that both systems are consistent for the most part during periods where the ABP signal is relatively stationary. The proposed algorithm has better performance than the commercial PPV monitoring system during periods of abrupt ABPM changes.

blood loss. These results indicate that while the PICCO system is a useful tool to estimate PPV and predict fluid responsiveness in situations where normal hemodynamic changes are expected, it may not provide accurate PPV values in certain situations.

As shown in Figs. 1 and 2, the proposed algorithm is capable of accurately estimating the PPV index during periods of significant hemodynamic changes and is robust to artifact. Note that in all the subjects, the PPV estimates obtained with the algorithm are consistent with the PPV expert annotations.

Table II provides a quantitative measure of the difference in performance of the PICCO system and the proposed algorithm both before and after post-filtering, by providing the absolute error for each estimate versus the corresponding “gold-standard” data point for all 18 subjects. As mentioned earlier, the PICCO system performs well during normal changes in hemodynamics. This is illustrated by the low absolute error reported for points 1 and 5 on all subjects in the table. However, during periods of rapid hemodynamic changes (points 2–4), the absolute error is much larger for the PICCO system estimate than the proposed algorithm. Furthermore, the overall absolute error over all subjects is 2083.19 for the PICCO system, which is nearly four times greater than the error of 555.18 from the proposed algorithm.

Our results show that the new enhanced algorithm to estimate PPV improves the performance of our previously published algorithm adopted by Philips Medical Systems as part of their Intellivue MP70 Monitors. The previous algorithm has already been thoroughly validated in a clinical study and has been found to be both accurate and useful in clinical environments. However, there is a need to improve upon this algorithm currently implemented as part of a commercial system, particularly to

make it more robust to artifact and accurate during regions of abrupt hemodynamic changes.

As mentioned in Section I, despite the availability of a commercial devices for PPV monitoring, the need for additional independent PPV estimation algorithms are significant for several reasons. Researchers have found that these commercial systems are not always accurate. This is the case in this situation. Additionally, the enhanced algorithm presented in this paper can be implemented and used to estimate PPV in data already collected. We provide a detailed description to ensure that other researchers and manufacturers can implement and use it for research purposes and independently validate the results obtained using commercial PPV monitoring systems.

A. Study Limitations

Instead of the typical statistical results (and Bland–Altman plots), in our results, we document the absolute error for each point and time domain plots, since it is important to capture how the algorithms perform at each instance after the transient response. For instance, it is important to know whether the algorithms fail after the high-to-low or during the low-to-high BP transitions. Consequently, we decided to report the results of the absolute error at each time instant and corresponding time-domain plots of the transient characteristics, since this provides more information to assess where the algorithms have more difficulty estimating PPV during abrupt hemodynamic changes. The typical methodology employed for clinical validation of PPV algorithms is not appropriate in this case since it does not provide information regarding failures due to abrupt hemodynamic changes.

TABLE II
COMPARISON OF THE PICCO SYSTEM VERSUS THE PROPOSED ALGORITHM BEFORE (PPU) AND AFTER (PPF) POSTFILTERING AGAINST THE GOLD-STANDARD PPV MANUALLY ANNOTATED BY TRAINED EXPERTS SHOWING THE ABSOLUTE ERROR

Subject	Point	Gold Standard	PICCO [®]	Proposed (PPU)	Proposed (PPF)	Absolute Error (PICCO) [®]	Absolute Error (PPU)	Absolute Error (PPF)
1	1	15.75	18	18.33	15.75	2.25	2.58	0
.	2	45.33	27	46.17	46.9	18.33	0.84	1.57
.	3	56	22	70.93	71.91	34	14.93	15.91
.	4	45.86	28	46.15	48.63	17.86	0.29	2.77
.	5	5.856	7	7.574	7.7	1.144	1.718	1.844
2	1	16.35	22	23	23	5.65	6.65	6.65
.	2	55.74	26	63.65	54	29.74	7.91	1.74
.	3	43.12	18	54.75	53.04	25.12	11.63	9.92
.	4	34.94	23	43.68	45.14	11.94	8.74	10.2
.	5	13.22	11	15.81	14.96	2.22	2.59	1.74
3	1	12.98	15	16.19	15.32	2.02	3.21	2.34
.	2	47.92	33	55.08	54.08	14.92	7.16	6.16
.	3	52.97	26	53.5	54.1	26.97	0.53	1.13
.	4	9.001	6	7.347	8.033	3.001	1.654	0.968
.	5	3.448	5	7.298	6.554	1.552	3.85	3.106
4	1	10.32	18	18.47	17.11	7.68	8.15	6.79
.	2	59.85	33	56.51	54.67	26.85	3.34	5.18
.	3	70.9	-1	69.54	68.27	71.9	1.36	2.63
.	4	59.57	-1	56.91	49.16	60.57	2.66	10.41
.	5	14.36	-1	43.62	38.05	15.36	29.26	23.69
5	1	6.357	15	18.57	19.48	8.643	12.213	13.123
.	2	50.85	37	63.66	62.17	13.85	12.81	11.32
.	3	60.38	-1	66.9	69.3	61.38	6.52	8.92
.	4	60.04	29	64.65	66.23	31.04	4.61	6.19
.	5	13.36	-1	22.11	18.61	14.36	8.75	5.25
6	1	16.74	17	14.68	22.14	0.26	2.06	5.4
.	2	36.97	33	60.03	57.19	3.97	23.06	20.22
.	3	63.21	29	64.8	64.66	34.21	1.59	1.45
.	4	58.63	26	62.24	64.16	32.63	3.61	5.53
.	5	12.87	12	11.37	12.08	0.87	1.5	0.79
7	1	15.35	17	16.93	17.92	1.65	1.58	2.57
.	2	55.7	36	47.83	51.6	19.7	7.87	4.1
.	3	47.93	30	47.99	49.09	17.93	0.06	1.16
.	4	56.34	-1	51.8	53	57.34	4.54	3.34
.	5	19.48	18	21.06	16.61	1.48	1.58	2.87
8	1	14.86	14	18.17	21.07	0.86	3.31	6.21
.	2	53.73	22	70.75	62.24	31.73	17.02	8.51
.	3	41.9	32	46.34	45.38	9.9	4.44	3.48
.	4	6.625	12	15.71	12.26	5.375	9.085	5.635
.	5	8.981	9	14.87	10.26	0.019	5.889	1.279
9	1	25.21	19	26.65	22.73	6.21	1.44	2.48
.	2	108.2	10	90.89	85.86	98.2	17.31	22.34
.	3	60.42	29	62.53	60.08	31.42	2.11	0.34
.	4	59.15	36	54.29	52.32	23.15	4.86	6.83
.	5	14.69	13	15.24	14.94	1.69	0.55	0.25
10	1	21.69	9	14.42	16.54	12.69	7.27	5.15
.	2	74.49	17	73.63	64.33	57.49	0.86	10.16
.	3	60.59	27	51.7	55.13	33.59	8.89	5.46
.	4	58.87	26	61.87	65.25	32.87	3	6.38
.	5	10.77	9	11.23	11.53	1.77	0.46	0.76
11	1	11.16	13	15.52	26.87	1.84	4.36	15.71
.	2	58.26	-1	68.35	78.22	59.26	10.09	19.96
.	3	70.87	15	59.62	54.16	55.87	11.25	16.71
.	4	11.93	15	21.6	16.45	3.07	9.67	4.52
.	5	6.583	7	7.682	8.101	0.417	1.099	1.518
12	1	20.68	18	19.82	24.74	2.68	0.86	4.06
.	2	75	20	75.37	74.55	55	0.37	0.45
.	3	71.9	-1	66.43	71.2	72.9	5.47	0.7
.	4	35.16	-1	47.34	59.17	36.16	12.18	24.01
.	5	22.13	19	32.45	31.64	3.13	10.32	9.51
13	1	21.17	-1	23.28	24.27	22.17	2.11	3.1
.	2	49.3	25	73.3	66.37	24.3	24	17.07
.	3	68.12	24	74.88	59.57	44.12	6.76	8.55
.	4	60.8	28	62.69	55.68	32.8	1.89	5.12
.	5	17.79	19	19.92	18.14	1.21	2.13	0.35
14	1	16.92	13	16.63	16.03	3.92	0.29	0.89
.	2	75.29	-1	78.16	71.85	76.29	2.87	3.44
.	3	80.11	-1	56.73	70.53	81.11	23.38	9.58
.	4	9.257	13	11.85	10.21	3.743	2.593	0.953
.	5	6.61	6	5.409	6.046	0.61	1.201	0.564
15	1	11.08	13	14.65	16.34	1.92	3.57	5.26
.	2	61.14	-1	82.41	65.73	62.14	21.27	4.59
.	3	67.11	28	63	62.13	39.11	4.11	4.98
.	4	54.44	-1	60.47	59.86	55.44	6.03	5.42
.	5	6.393	10	10.45	13.09	3.607	4.057	6.697
16	1	14.51	16	14.48	14.93	1.49	0.03	0.42
.	2	27.67	28	35.97	36.97	0.33	8.3	9.3
.	3	58.63	-1	57.83	60.82	59.63	0.8	2.19
.	4	47.81	29	55.36	49.83	18.81	7.55	2.02
.	5	13.53	11	12.91	12.16	2.53	0.62	1.37
17	1	13.65	14	9.585	12.28	0.35	4.065	1.37
.	2	67.35	-1	60.96	60.2	68.35	6.39	7.15
.	3	86.57	17	67.6	77.67	69.57	18.97	8.9
.	4	23.32	25	32.08	40.15	1.68	8.76	16.83
.	5	3.162	5	7.062	5.982	1.838	3.9	2.82
18	1	19.25	15	14.46	15.53	4.25	4.79	3.72
.	2	57.14	34	71.11	73.27	23.14	13.97	16.13
.	3	73.29	36	75.4	80.04	37.29	2.11	6.75
.	4	62.75	38	37.24	70.84	24.75	25.51	8.09
.	5	5.993	7	8.937	8.156	1.007	2.944	2.163
Total Absolute Error						2083.19	578.53	555.18

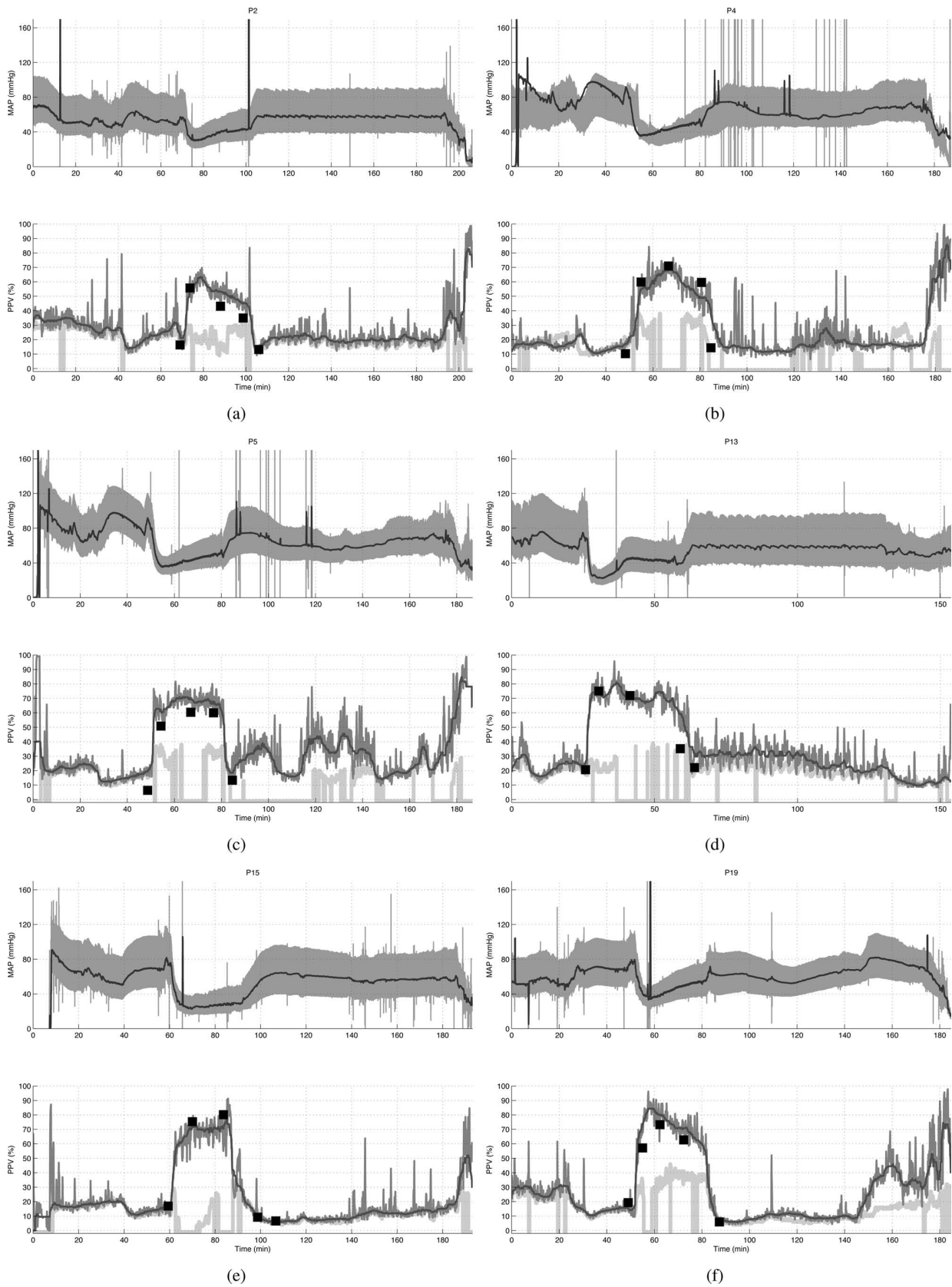


Fig. 2. Comparison of the proposed PPV algorithm (dark grey) against a commercial PPV monitoring system (light grey) for subjects listed in Table II. For each subject the top plot shows the ABP signal and the bottom plot shows the estimated PPV using both algorithms. Five “gold-standard” PPV manual annotations calculated by trained experts during periods of abrupt ABP changes are shown as black squares on the bottom plot of each subject. Note that both systems are consistent for the most part during periods where the ABP signal is relatively stationary. The proposed algorithm has better performance than the commercial PPV monitoring system during periods of abrupt ABPM changes.

The PICCO algorithm is proprietary and to our knowledge there is no published paper that thoroughly describes the algorithm used by the PICCO system. Since the algorithm implemented in the PICCO system has not been described in a manner that ensures reproducibility by the research community, we have not been able to implement it, and we do not know exactly how it estimates PPV or whether the required calibration for cardiac output impacts the PPV. The PPV PICCO results presented in this paper were obtained directly using the PiCCO system.

An important point to emphasize is that both the PICCO system and our algorithms are trying to estimate PPV (as defined by the PPV formula). However, this formula cannot be computed automatically, and consequently, a complex algorithm must be used to get the best "estimate" of PPV. It is the algorithms used to estimate PPV that are different, not the formula used to define PPV.

V. CONCLUSION

In this paper, we described a new enhanced algorithm to estimate PPV that improves the performance of our previously published algorithm adopted by Philips Medical Systems as part of their Intellivue MP70 Monitors. The previous algorithm has already been thoroughly validated in a clinical study and has been found to be both accurate and clinically useful. However, there is a need to improve upon this algorithm currently implemented as part of a commercial system, particularly to make it more robust to artifact and accurate during regions of abrupt hemodynamic changes. Estimation of PPV is a very significant problem, since PPV has been found to be one of the best predictors of fluid responsiveness. Despite the significance of PPV, currently there are no publicly available validated algorithms that can be used to estimate it on recorded ABP signals. Additionally, commercial hemodynamic monitoring systems with PPV monitoring capabilities may not work well during regions of abrupt hemodynamic changes. This paper has three main contributions: 1) a description of a robust new method to estimate PPV from ABP signals, 2) the assessment of the robustness of the PICCO system during regions of abrupt hemodynamic changes, and 3) a prospective validation and comparison of the proposed algorithm against the PICCO system.

Our validation results indicate that this algorithm has superior performance compared to commercial hemodynamic monitoring systems with PPV capabilities. The assessment results show that the proposed algorithm is capable of accurately estimating the PPV index during periods of significant hemodynamic changes. The commercial system used as a benchmark failed to accurately estimate the PPV during these periods. Additionally, our proposed PPV algorithm can be implemented and used to estimate PPV in data already collected and archived.

It is important to emphasize that a clinical validation study assessing the ability of the proposed enhanced algorithm to monitor fluid responsiveness in the operating room in situations involving abrupt hemodynamic changes still needs to be conducted. This would require the proposed algorithm to be first adopted as part of a commercial system as was the case with the underlying automatic PPV algorithm.

ACKNOWLEDGMENT

The authors would like to acknowledge Dr. C. Phillips from Oregon Health and Science University for providing the data used to validate the proposed algorithm and assess its performance during regions of abrupt hemodynamic change.

REFERENCES

- [1] F. Michard, "Changes in arterial pressure during mechanical ventilation," *Anesthesiology*, vol. 103, no. 2, pp. 419–428, Aug. 2005 (quiz 449-5).
- [2] C. K. Hofer, L. Furrer, S. Matter-Ensner, M. Maloigne, R. Klaghofer, M. Genoni, and A. Zollinger. (2005, Jun.). Volumetric preload measurement by thermodilution: A comparison with transoesophageal echocardiography. *Brit. J. Anaesth.* [Online]. 94(6), pp. 748–755. Available: <http://dx.doi.org/10.1093/bja/aei123>
- [3] F. Michard, S. Boussat, D. Chemla, N. Anguel, A. Mercat, Y. Lecarpentier, C. Richard, M. R. Pinsky, and J. L. Teboul, "Relation between respiratory changes in arterial pulse pressure and fluid responsiveness in septic patients with acute circulatory failure," *Amer. J. Respir. Crit. Care Med.*, vol. 162, no. 1, pp. 134–138, Jul. 2000.
- [4] F. Michard, L. Ruscio, and J. L. Teboul, "Clinical prediction of fluid responsiveness in acute circulatory failure related to sepsis," *Intensive Care Med.*, vol. 27, no. 7, p. 1238, Jul. 2001.
- [5] A. Kramer, D. Zygun, H. Hawes, P. Easton, and A. Ferland. (2004, Nov.). Pulse pressure variation predicts fluid responsiveness following coronary artery bypass surgery. *Chest* [Online]. 126(5), pp. 1563–1568. Available: <http://dx.doi.org/10.1378/chest.126.5.1563>
- [6] F. Michard and J.-L. Teboul, "Predicting fluid responsiveness in ICU patients: A critical analysis of the evidence," *Chest*, vol. 121, no. 6, pp. 2000–2008, Jun. 2002.
- [7] M. Aboy, J. McNames, T. Thong, C. R. Phillips, M. S. Ellenby, and B. Goldstein, "A novel algorithm to estimate the pulse pressure variation index deltaPP," *IEEE Trans. Biomed. Eng.*, vol. 51, no. 12, pp. 2198–2203, Dec. 2004.
- [8] M. Cannesson, J. Sliker, O. Desebbe, C. Bauer, P. Chiari, R. Hénaïne, and J.-J. Lehot. (2008, Apr.). The ability of a novel algorithm for automatic estimation of the respiratory variations in arterial pulse pressure to monitor fluid responsiveness in the operating room. *Anesth. Analg.* [Online]. 106(4), pp. 1195–1200. Available: <http://dx.doi.org/10.1213/01.ane.0000297291.01615.5c>
- [9] M. Cannesson, C. Bionda, B. Gostoli, O. Raïsky, S. di Filippo, D. Bompard, C. Védrette, R. Rousson, J. Ninet, J. Neidecker, and J.-J. Lehot. (2007, May). Time course and prognostic value of plasma b-type natriuretic peptide concentration in neonates undergoing the arterial switch operation. *Anesth. Analg.* [Online]. 104(5), pp. 1059–1065. Available: <http://dx.doi.org/10.1213/01.ane.0000263644.98314.e2>
- [10] M. Cannesson, O. Desebbe, P. Rosamel, B. Delannoy, J. Robin, O. Bastien, and J.-J. Lehot. (2008, Aug.). Pleth variability index to monitor the respiratory variations in the pulse oximeter plethysmographic waveform amplitude and predict fluid responsiveness in the operating theatre. *Brit. J. Anaesth.* [Online]. 101(2), pp. 200–206. Available: <http://dx.doi.org/10.1093/bja/aen133>
- [11] M. Cannesson, R. Hénaïne, S. D. Filippo, J. Neidecker, D. Bompard, C. Védrette, and J.-J. Lehot. (2008, Oct.). Clinical usefulness of new-generation pulse oximetry in the paediatric cardiac surgery setting. *Ann. Fr. Anesth. Reanim.* [Online]. Available: <http://dx.doi.org/10.1016/j.annfar.2008.06.012>
- [12] J. Bajorat, R. Hofmockel, D. A. Vagts, M. Janda, B. Pohl, C. Beck, and G. Noeldge-Schomburg. (2006, Jan.). Comparison of invasive and less-invasive techniques of cardiac output measurement under different haemodynamic conditions in a pig model. *Eur. J. Anaesthesiol.* [Online]. 23(1), pp. 23–30. Available: <http://dx.doi.org/10.1017/S0265021505001717>
- [13] H. Berkenstadt, N. Margalit, M. Hadani, Z. Friedman, E. Segal, Y. Villa, and A. Perel, "Stroke volume variation as a predictor of fluid responsiveness in patients undergoing brain surgery," *Anesth. Analg.*, vol. 92, no. 4, pp. 984–989, Apr. 2001.
- [14] A. Combes, J.-B. Berneau, C.-E. Luyt, and J.-L. Trouillet. (2004, Jul.). Estimation of left ventricular systolic function by single transpulmonary thermodilution. *Intensive Care Med.* [Online]. 30(7), pp. 1377–1383. Available: <http://dx.doi.org/10.1007/s00134-004-2289-2>
- [15] C. K. Hofer, S. M. Müller, L. Furrer, R. Klaghofer, M. Genoni, and A. Zollinger. (2005, Aug.). Stroke volume and pulse pressure variation

for prediction of fluid responsiveness in patients undergoing off-pump coronary artery bypass grafting. *Chest* [Online]. 128(2), pp. 848–854. Available: <http://dx.doi.org/10.1378/chest.128.2.848>

[16] M. V. Küntscher, S. Blome-Eberwein, M. Pelzer, D. Erdmann, and G. Germann, “Transcardiopulmonary vs pulmonary arterial thermodilution methods for hemodynamic monitoring of burned patients,” *J. Burn Care Rehabil.*, vol. 23, no. 1, pp. 21–26, 2002.

[17] C. Kuhn, A. Kuhn, K. Rykow, and B. Osten. (2006, Jan.). Extravascular lung water index: A new method to determine dry weight in chronic hemodialysis patients. *Hemodial. Int.* [Online]. 10(1), pp. 68–72. Available: <http://dx.doi.org/10.1111/j.1542-4758.2006.01177.x>

[18] J.-M. Liet, C. Jacqueline, J.-L. Orsonneau, C. Gras-Leguen, G. Potel, and J.-C. Rozé. (2005, Mar.). The effects of milrinone on hemodynamics in an experimental septic shock model. *Pediatr. Crit. Care Med.* [Online]. 6(2), pp. 195–199. Available: <http://dx.doi.org/10.1097/01.PCC.0000155636.53455.96>

[19] G. Padua, G. Canestrelli, G. Pala, D. Sechi, and M. C. Spanu, “Original insight into continuous cardiac output monitoring: “TruCCOMS” Correlation with other methods,” *Minerva Anesthesiol.*, vol. 69, no. 7/8, pp. 617–624, 2003.

[20] G. D. Rocca, M. G. Costa, C. Coccia, L. Pompei, and P. Pietropaoli, “Preload and haemodynamic assessment during liver transplantation: A comparison between the pulmonary artery catheter and transpulmonary indicator dilution techniques,” *Eur. J. Anaesthesiol.*, vol. 19, no. 12, pp. 868–875, Dec. 2002.

[21] G. D. Rocca, M. G. Costa, L. Pompei, C. Coccia, and P. Pietropaoli, “Continuous and intermittent cardiac output measurement: pulmonary artery catheter versus aortic transpulmonary technique,” *Brit. J. Anaesth.*, vol. 88, no. 3, pp. 350–356, Mar. 2002.

[22] G. D. Rocca, M. G. Costa, C. Coccia, L. Pompei, P. D. Marco, and P. Pietropaoli, “Preload index: Pulmonary artery occlusion pressure versus intrathoracic blood volume monitoring during lung transplantation,” *Anesth. Analg.*, vol. 95, no. 4, pp. 835–843, Oct. 2002.

[23] G. D. Rocca, M. G. Costa, C. Coccia, L. Pompei, P. D. Marco, V. Vilardi, and P. Pietropaoli, “Cardiac output monitoring: Aortic transpulmonary thermodilution and pulse contour analysis agree with standard thermodilution methods in patients undergoing lung transplantation,” *Can. J. Anaesth.*, vol. 50, no. 7, pp. 707–711, 2003.

[24] C. Romero, M. Andresen, O. Díaz, V. Tomicic, F. Baraona, M. Mercado, C. Pérez, P. Downey, and A. Dougnac, “Hantavirus cardiopulmonary syndrome: Utility of the PICCO (pulse contour cardiac output) system for monitoring,” *Rev. Med. Chil.*, vol. 131, no. 10, pp. 1173–1178, Oct. 2003.

[25] M. Rupérez, J. López-Herce, C. García, C. Sánchez, E. García, and D. Vigil. (2004). Comparison between cardiac output measured by the pulmonary arterial thermodilution technique and that measured by the femoral arterial thermodilution technique in a pediatric animal model, *Pediatr. Cardiol.* [Online]. 25(2), pp. 119–123. Available: <http://dx.doi.org/10.1007/s00246-003-0450-2>

[26] A. Torgay, A. Pirat, E. Akpek, P. Zeyneloglu, G. Arslan, and M. Haberal. (2005, Sep.). Pulse contour cardiac output system use in pediatric orthotopic liver transplantation: Preliminary report of nine patients. *Transplant Proc.* [Online]. 37(7), pp. 3168–3170. Available: <http://dx.doi.org/10.1016/j.transproceed.2005.07.020>

[27] F. Valenza, M. Irace, M. Guglielmi, S. Gatti, N. Bottino, C. Tedesco, M. Maffioletti, P. Maccagni, T. Fossali, G. Aletti, and L. Gattinoni. (2005, Jan.). Effects of continuous negative extra-abdominal pressure on cardiorespiratory function during abdominal hypertension: An experimental study. *Intensive Care Med.* [Online]. 31(1), pp. 105–111. Available: <http://dx.doi.org/10.1007/s00134-004-2483-2>

[28] J. M. J. Vizquete, M. C. Sáenz, R. P. García, M. A. Molina, J. C. García, and A. B. C. del Pozo, “PiCCO monitoring of 4 critically ill patients,” *Rev. Esp. Anesthesiol. Reanim.*, vol. 51, no. 3, pp. 158–163, Mar. 2004.

[29] C. Wiesenack, C. Fiegl, A. Keyser, C. Prasser, and C. Keyl, “Assessment of fluid responsiveness in mechanically ventilated cardiac surgical patients,” *Eur. J. Anaesthesiol.*, vol. 22, no. 9, pp. 658–665, Sep. 2005.

[30] N. X. Zhang, Y. Z. Qin, L. Xu, and S. P. Wang, “Clinical comparative study of airway pressure release ventilation and continuous positive airway pressure ventilation,” *Zhongguo Wei Zhong Bing Ji Jiu Yi Xue*, vol. 17, no. 8, pp. 481–483, Aug. 2005.

[31] M. Abov, J. McNames, T. Thong, D. Tsunami, M. S. Ellenby, and B. Goldstein, “An automatic beat detection algorithm for pressure signals,” *IEEE Trans. Biomed. Eng.*, vol. 52, no. 10, pp. 1662–1670, Oct. 2005.



Mateo Abov (M’98) was born in Pontevedra, Spain, in 1980. He received the B.S. degree (high honors) in electrical engineering and the B.S. degree (high honors) in physics with a minor in mathematics from Portland State University (PSU), Portland, OR, in 2002, the M.S. degree (*summa cum laude*) in electrical and computer engineering from PSU in 2004, and the M.Phil. (DEA) and Ph.D. (*summa cum laude*) degrees from the School of Telecommunications Engineers (ETSIT-Vigo), University of Vigo, Vigo, Spain, in 2004 and 2005, respectively. He is currently working toward the MBA degree at the University of London, London, U.K.

He completed the Executive Certificate Program in management and leadership with a focus on technical management from the Massachusetts Institute of Technology (MIT) Sloan School of Management in 2007 and graduate/professional coursework in IP law from the University of California, Berkeley, in 2007. He has a Bar Admission to practice patent law before the United States Patent and Trademark Office and was a Managing Partner and a Patent Agent at Abov&Associates PC (www.abovpatentlaw.com). Since 2005, he has been with the Oregon Institute of Technology (OIT), Portland. He is currently a tenure Associate Professor and the Department Chair of the Electrical Engineering Department (EERE), and holds joint appointments at University of Vigo (Doctoral Program in Signal Processing) and Biomedical Engineering Division, School of Medicine, Oregon Health and Science University. His current research interests include practical applications of signal processing. He has authored or coauthored over 60 scholarly articles and international conference proceedings papers, including 12 journal papers in the IEEE TRANSACTIONS ON BIOMEDICAL ENGINEERING.

Dr. Abov was an Associate Editor and Scientific Committee Member for the IEEE-Revista Iberoamericana de Tecnologías del Aprendizaje (RITA) Journal, an Associate Editor for the IEEE Engineering in Medicine and Biology Conference, and the President (Chair) of the IEEE Education Society in Oregon. He is a Full Member of the Scientific Research Society (Sigma XI), a Lifetime Honorary Member of the Golden-Key Honor Society, a past Chapter President of HKN (International Electrical Engineering Honor Society), and a past Corresponding Secretary of TBP (National Engineering Honor Society). He is a licensed Professional Engineer in Spain, European Union.



Cristina Crespo received the B.S. degree (high honors) in electrical engineering and the B.S. degree (high honors) in physics with a minor in mathematics from Portland State University (PSU), Portland, OR, in 2002, the M.S. degree (*summa cum laude*) in electrical and computer engineering from PSU in 2004, and the M.Phil (DEA) degree from the School of Telecommunications Engineers (ETSIT-Vigo), University of Vigo, Vigo, Spain, in 2009. She is currently working toward the Ph.D. degree in electrical engineering at ETSIT-Vigo.

From 2003 to 2008, she was an Electrical Engineer as part of the High Speed Signal Processing/Signal Sensing and Interconnect Products Business Unit, Maxim Integrated Products, Inc. In 2009, she joined the Electrical Engineering Department (EERE), Oregon Institute of Technology (OIT), Portland.



Daniel Austin (M’09) received the B.S. degree in electronics engineering technology from the Oregon Institute of Technology (OIT), Portland, in 2006, and the M.S. degree in electrical engineering from the University of Southern California, Los Angeles, in 2008. He is currently working toward the Ph.D. degree in electrical engineering at Portland State University (PSU), Portland.

From 2005 to 2008, he was an Electrical Engineer at Maxim Integrated Products, Inc. Since 2008, he has been a Research Associate with the Biomedical Engineering Division, Oregon Health and Science University. His current research interests include statistical signal processing and modeling with applications to biomedical engineering.